Structural and Thermodynamic Studies on a Salt-bridge Triad in the NADP-binding Domain of Glutamate Dehydrogenase from *Thermotoga maritima*: Cooperativity and Electrostatic Contribution to Stability†

Joyce H. G. Lebbink,‡,§ Valerio Consalvi,|| Roberta Chiaraluce,|| Kurt D. Berndt,‡,⊥ and Rudolf Ladenstein*,‡

Center for Structural Biochemistry, Department of Biosciences at Novum, Karolinska Institutet, 14157 Huddinge, Sweden, Dipartimento di Scienze Biochimiche 'A Rossi Fanelli', Università 'La Sapienza', Piazzale A. Moro 5, 00185 Rome, Italy, and Faculty of Natural Sciences, Södertörns Högskola, 141 89 Huddinge, Sweden

Received July 8, 2002; Revised Manuscript Received October 16, 2002

ABSTRACT: Cooperative interactions within ion-pair networks of hyperthermostable proteins are thought to be a major determinant for extreme protein stability. While the favorable thermodynamic contributions of optimized electrostatics in general as well as those of pairwise interactions have been documented, cooperativity between pairwise interactions has not yet been studied thermodynamically in proteins from hyperthermophiles. In this study we use the isolated cofactor binding domain of glutamate dehydrogenase from the hyperthermophilic bacterium *Thermotoga maritima* to analyze pairwise and cooperative interactions within the salt-bridge triad Arg190−Glu231−Lys193. The X-ray structure of the domain was solved at 1.43 Å and reveals the salt-bridge network with surrounding solvent molecules in detail. All three participating charges in the network were mutated to alanine in all combinations. The X-ray structure of the variant lacking all three charges reveals that the removal of the side chains has no effect on the overall conformation of the protein. Using solvent denaturation and thermodynamic cycles, the interaction energies between each pair of residues in the network were determined in the presence and in the absence of the third residue. Both the Arg190−Glu231 ion pair and the Lys193-Glu231 salt bridge in the absence of the third residue, contribute favorably to the free energy for unfolding of the domain in urea. Using guanidinium chloride as denaturant reveals a strong cooperativity between the two ion-pair interactions, the presence of the second ion pair converts the first interaction from destabilizing into stabilizing by as much as 1.09 kcal/mol. The different energetics of the salt-bridge triad in urea and GdmCl are discussed with reference to the observed anion binding in the crystal structure at high ionic strength and their possible role in a highly charged, high-temperature environment such as the cytoplasm of hyperthermophiles.

On the basis of recent progress in comparative structural analysis, molecular dynamics, and biochemical and biophysical characterization of wild-type and mutant proteins from hyperthermophilic organisms, it is now becoming more apparent that charged amino acid residues and their arrangement into large networks play an important role in maintaining a stable and biologically active protein structure at high temperatures (*1*−*4*). Extensive networks of positively and negatively charged residues have been reported for example in glutamate dehydrogenases (GluDH) and lumazine synthase from hyperhermophiles (*5*−*9*). Initial mutagenesis studies on proteins from mesophiles have shown that exposed ion-pair interactions contribute only marginally to the stabilization free energy (*10*−*12*). It was argued that the gain in electrostatic energy upon formation of a salt bridge is offset by the entropic cost of desolvation and localization of the flexible side chains. However, at higher temperatures charged interactions become relatively more favorable and contribute more to protein stability. Due to a decreased desolvation penalty at higher temperature, the energy barrier to solvate an ion pair is higher, resulting in an increase in strength of electrostatic interactions. Molecular dynamics calculations have shown that at higher temperatures more energy is required to solvate and thereby disrupt a salt bridge while there is no such barrier for breaking the interaction between hydrophobic isosteres of charged amino acids (*13*).

Using site-directed mutagenesis, ion-pair interactions have been removed from or have been introduced into proteins from hyperthermophiles. In a few cases, these substitutions had no effect on the resistance of the proteins against heat

† This work was partly supported by Marie Curie Individual Fellowship Contract QLK3-CT-1999-51141 to J.L.

* Corresponding author. E-mail: rudolf.ladenstein@csb.ki.se. Phone: + 46 8 608 9222. Fax: + 46 8 608 9290.

‡ Karolinska Institutet.

§ Present address: Department of Molecular Carcinogenesis, Netherlands Cancer Institute, Plesmanlaan 121, 1066 CX Amsterdam, The Netherlands.

|| Università 'La Sapienza'.

⊥ Södertörns Högskola.

[1] Abbreviations: CD, circular dichroism; DTT, dithiotreitol; EDTA, ethylenediaminetetraacetic acid; GdmCl, guanidinium chloride; GluDH, glutamate dehydrogenase; rmsd, root-mean-square deviation. Arg190/Ala193/Ala231 refers to the protein variant with an arginine at position 190, alanine at position 193, and alanine at position 231. Other protein variants are described accordingly.

10.1021/bi020461s CCC: $22.00
Published on Web 12/05/2002

inactivation or denaturation (*14*, *15*). In other studies, ion pairs and their arrangement into networks were shown to play an important role in protein stabilization (*16*−*20*). However, due to the irreversible inactivation and denaturation of these large, multimeric enzymes, a thermodynamic analysis of the results has not been possible and the extent of contribution by electrostatic interactions to the stability of proteins from hyperthermophiles remained elusive. Nevertheless, in most studies the importance of the correct context into which a potential stabilizing interaction was introduced, was pointed out. This was also noted by Spassov and co-workers who used a database survey to show that proteins in general gain electrostatic stabilization by minimizing the number of repulsive contacts (*21*). Proteins from hyperthermophiles gain further stability by additionally increasing the number of attractive electrostatic interactions (*22*). Stabilization of proteins by optimizing charge−charge interactions on the protein surface was recently demonstrated on ubiquitin and a 41-residue helical protein (*23*, *24*). Differences in protein environment around salt bridges in GluDH and other protein families determine to what extent these interactions contribute to protein stability (*25*, *26*). Optimized electrostatics are also the major determinant of thermal stability in a family of small cold-shock proteins (*27*). Enhanced stability in this family is achieved mainly by a single amino acid replacement that improves the electrostatic interactions among the charged groups on the protein surface in a delocalized manner, that is, in the absence of any attractive pairwise interaction (*27*−*29*).

Pairwise interactions have been shown to contribute to the free unfolding energies of hyperthermostable proteins. In *Pyrococcus furiosus* rubredoxin, a stabilizing pairwise interaction energy between a glutamate and the N-terminus was determined using double mutant cycles (*30*). In the cold-shock protein family, thermostabilization is achieved by removal of pairwise repulsive interactions between exposed glutamate residues (*28*).

In proteins from mesophiles, a typical characteristic of salt-bridge interactions is that they may contribute in a cooperative way to stability, protein folding, and protein-inhibitor interactions (*10*, *31*, *32*). For protein stability this phenomenon means that a particular salt-bridge interaction is strengthened by one of its partners being involved in a second ion-pair interaction. A first indication for cooperative interactions in large salt-bridge networks in a protein from a hyperthermophile came from the mutagenesis on a subunit interface ion-pair network in *Thermotoga maritima* GluDH. Nonadditivity was observed by combination of three destabilizing mutations in a mutant protein that was more resistant against thermal inactivation and denaturation than the wild-type GluDH (*19*). Cooperativity between salt-bridge clusters on the surface of the DNA-binding protein Sac7d from the hyperthermophile *Sulfolobus acidocaldarius* was suggested by molecular dynamics simulations (*33*). In the present study, we aim to provide evidence for cooperativity in salt-bridge networks in hyperthermostable proteins and to quantify this cooperative interaction.

GluDH is the model system we employ to study the role of ion-pair networks in hyperthermostable enzymes. GluDH is in general a hexameric enzyme, consisting of identical subunits containing a substrate and a cofactor binding domain, that, on the basis of structural analyses, seem to form relatively independent folding units. This was also suggested by a domain-swapping study between two GluDHs, in which a cofactor binding from a mesophilic GluDH coupled to the glutamate binding domain from a hyperthermostable GluDH retained all its parental properties (*34*). This prompted us to investigate the possibilities of using this cofactor binding domain to study reversible unfolding thermodynamics of a hyperthermostable enzyme (*35*). The isolated GluDH cofactor binding domain from the hyperthermophilic bacterium *T. maritima* is a soluble, monomeric protein that undergoes reversible and cooperative thermal and chemical unfolding around neutral pH. In the present study, we have determined the three-dimensional X-ray structures of the isolated domain and a mutant variant to assess correct protein folding, their structural identity, and the presence of a three-residue ion-pair network. The strength and cooperativity of the interactions in this ion-pair network are studied using site-directed mutagenesis, chemical denaturation, and multiple thermodynamic cycles.

MATERIALS AND METHODS

Site-Directed Mutagenesis and Purification of GluDH Domain Variants. Using the overlap extension method (*36*), mutations were introduced into the gene fragment coding for the cofactor binding domain of the *Thermotoga maritima* glutamate dehydrogenase (*35*). The correct introduction of mutations and the DNA sequence of the complete gene fragments was verified by DNA sequencing. *Escherichia coli* BL21(DE3), containing wild-type or mutant variants of the expression plasmid, was cultured until an optical density at 600 nm of 0.8 was reached. Expression was induced at this point by addition of 1 mM final concentration of isopropylthiogalactoside and further incubation at 37 °C overnight. Cells were harvested, and proteins were purified essentially as described before (*35*), except for preparative Superose 12 column chromatography being exchanged for preparative Superdex 75 column chromatography and the anion exchange procedure being performed before the gel filtration step using DEAE sepharose (all materials from Amersham-Pharmacia Biotech). Pure GluDH domains were stored at 4 °C in the presence of 0.02% sodium azide. Protein concentrations were determined using extinction coefficients calculated according to (*37*).

Crystallization, Data Collection, and Structure Refinement. Protein samples were dialyzed against 20 mM Tris pH 7.5 (+1 mM DTT in the case of wild-type GluDH domain). Using the sitting drop vapor diffusion method, initial crystallization conditions were identified by a random screening protocol (*38*). Two microliters of protein solution (20 mg/mL) was mixed with 2 μL of reservoir solution. Inital conditions were optimized using a finer grid search. The final crystallization conditions for the wild-type GluDH domain were 100 mM sodium acetate pH 4.6, 3 M NaCl, and 1 mM DTT. Small crystals belonging to spacegroup $P2_12_12_1$ were obtained (Table 1). For data collection at beamline X11 at the synchrotron facility DESY (EMBL outstation Hamburg), a crystal was dipped in crystallization solution containing 25% glycerol and flash-frozen at 100 K using liquid nitrogen. Data were indexed, merged, and scaled using the HKL package (*39*). Phases were obtained by the molecular replacement procedure AMoRe (*40*) using the coordinates from residues A185 to A337 from the hexameric *T. maritima*

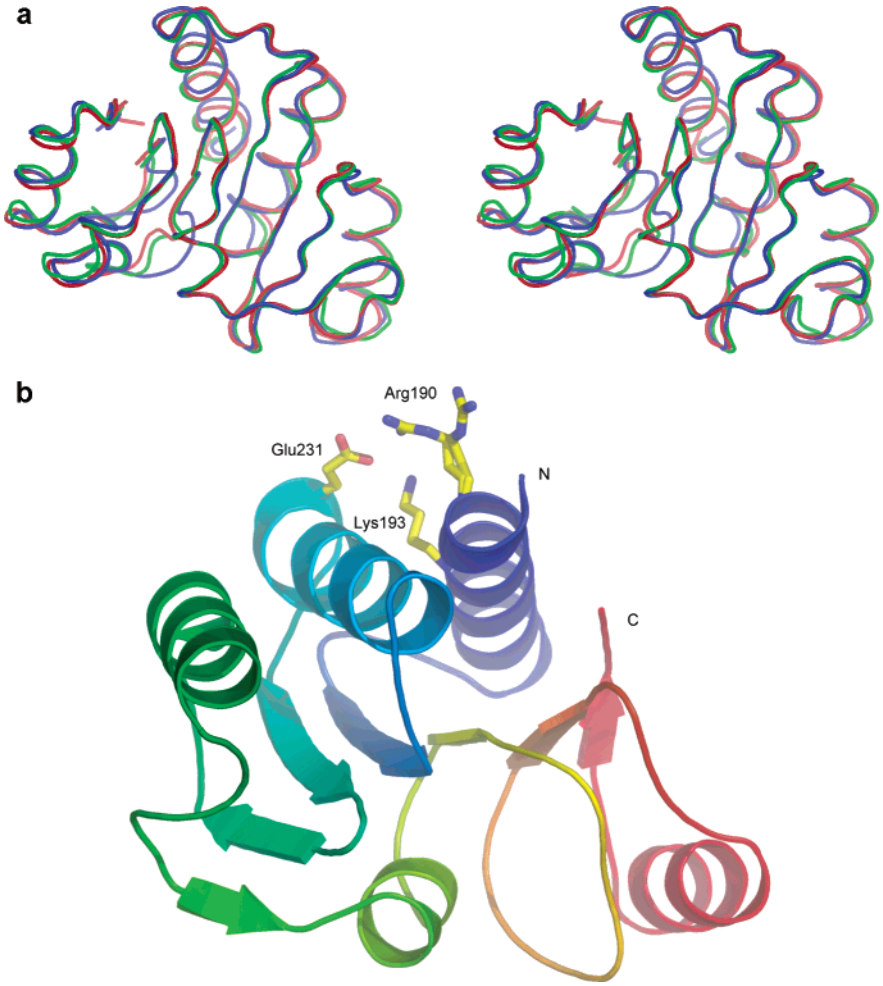

FIGURE 1: (a) Stereo image showing a superposition of subunit A from hexameric *Thermotoga maritima* GluDH (blue; PDB accession code 1B26; *7*), the isolated cofactor binding domain (red, this study), and variant Ala190/Ala193/Ala231 (green, this study). Rmsd between the domain as part of the hexamer and the isolated domain is 0.956 Å. Rmsd between the wild-type isolated domain and Ala190/Ala193/Ala231 is 0.560 Å. (b) Ribbon model of wild-type cofactor binding domain from *Thermotoga maritima* showing the central β-sheet surrounded on both sides by α-helices. Color coding runs from blue at the N-terminal region to red at the C-terminal region. The side chains of the three residues forming the salt-bridge triad (Arg190 in alternate conformations) are depicted as stick models with carbon atoms in yellow, oxygen in red, and nitrogen in blue. Figures were prepared using Pymol (*68*).

GluDH structure as search model (PDB accession code 1B26; *7*). The hexameric numbering of the residues was kept in the model of the isolated domain to allow direct comparison between corresponding residues in the two proteins. Initial refinement consisted of simulated annealing carried out with CNSsolve (*41*), using isotropic atomic displacement factors and a starting temperature of 5000 K. The initial *R*-factor of 49.5% dropped to 38.8% for the working set and 41.8% for the test set (5% of the reflections). Following this, restrained maximum likelihood refinement using Refmac (*42*, *43*) reduced the *R*-factor to 32.0% (R_{free} 37.1%). During alternate rounds of manual model building in O (*44*) and refinement using refmac (Refmac5 and the CCP4 graphical interface during later stages), anisotropic atomic displacement factors were refined and solvent was built using Arp (*45*). Considering the 3.0 M NaCl concentration in the crystallization setups, two peaks (CL2 and CL3 in the final model) in the electron density maps were assigned to chloride ions on the basis of the following criteria: (i) a σ value higher than 7 in a $2F_o-F_c$ map, (ii) residual positive density in an F_o-F_c difference map contoured at 3.0 σ when oxygen was built in, (iii) no negative density in the F_o-F_c map when Cl^- was built in, (iv) coordination by a positively charged side chain, and (v)

Table 1: Statistics on Data Collection and Refinement of Wild-type and Mutant *Thermotoga maritima* Isolated Cofactor Binding Domain

	wild-type	Ala190/Ala193/Ala231
(A) Crystal and Diffraction Data		
crystal cell dimensions (Å)	$a = 43.0$	$a = 68.0$
	$b = 44.1$	$b = 68.0$
	$c = 71.9$	$c = 60.7$
max. resolution	1.43 Å	2.6 Å
space group	$P2_12_12_1$	$P4_12_12$
completeness (last shell)	98.4% (96.7%)	99.8% (100%)
R_{merge}	5.1%	8.7%
no. of reflections (unique)	218 419 (25567)	126 931 (4703)
(B) Results of the Refinement		
R-factor	15.2%	24.8%
R_{free} factor	19.0%	29.2%
rmsd		
bond lengths (Å)	0.018	0.007
bond angles (deg)	1.789	1.206
dihedral angles (deg)	15.5	22.1
no. of amino acids	151	150
no. of atoms (non-hydrogens)	1251	1109
no. of solvent molecules	130	17
ramachandran; % residues in		
most favored regions	93.4	88.7
additional allowed regions	6.6	10.5
generously allowed regions	0.0	0.8
average *B*-factor all atoms (Å^2)	17.8	41.8

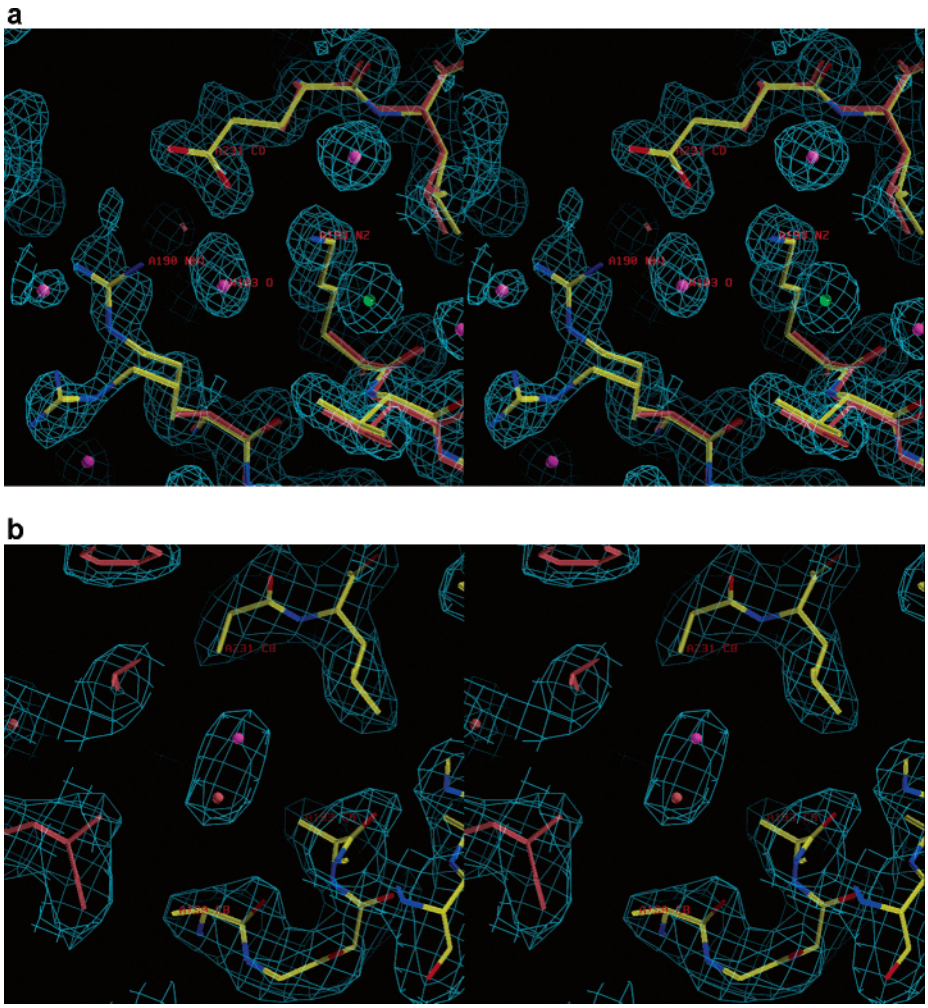

FIGURE 2: (a) Stereo diagram of a $2F_o-F_c$ map of the region of the salt-bridge triad in wild-type cofactor binding domain. Shown in yellow are the well-ordered side chains of Glu231 and Lys193 and the double conformation of Arg110 of the wild-type model. Central in the picture is solvent molecule W103 (purple). Furthermore, chloride W2 (green), coordinated by Lys193, is clearly visible. Superimposed in dark orange is the model of domain variant Ala190/Ala193/Ala231. (b) Stereo diagram of a $2F_o-F_c$ map of the region of the salt-bridge triad in domain variant Ala190/Ala193/Ala231. In yellow the model for the alanine residues is shown in exactly the same orientation as in the superposition in Figure 1a. Central in the picture is the solvent molecule (purple) next to the crystallographic 2-fold axis, which runs almost perpendicular to the plane of the picture. The solvent molecule and residues from a symmetry related molecule are shown in dark orange. Both maps were contoured at 1.0 σ, and the pictures were drawn with O (*44*).

B-factors similar to those of neighboring groups. Solvent atoms W10, W31, and W103 have been assigned to H_2O because of lower sigma values; however, they display positive densities in the F_o-F_c difference map and are all coordinated by positively charged side chains. Occupancies of protein atoms, for which no or only weak density was observed, were adjusted. No density at all was observed for the N-terminal 2 residues, which consequently have been removed from the model. Weak density was observed for an additional N-terminal residue and the C-terminal aspartate, as well as three residues in the loop Gly314−Ala315−Asn316, that in the hexamer pack against residues from the substrate-binding domain. The side chain of arginine 190 clearly adopted two different conformations, these were both modeled at 50% occupancy. The quality of the final model was checked using procheck (*46*) and WHATIF (*47*, *48*). The final model has excellent stereochemistry and an *R*-factor of 15.2% (R_{free} = 19.0%).

The final crystallization conditions for the Ala190/Ala193/Ala231 domain variant were 50 mM bis-tris-propane pH 6.5, 38% dioxane, and 25% glycerol. Small crystals were obtained that belonged to spacegroup $P4_12_12$ (Table 1). For data collection using a rotating anode and Cu κ_α radiation, a crystal was flash-frozen directly at 105 K. Phases for this mutant were determined using the coordinates of the final model for the isolated domain (described above) as search model with the single cysteine residue mutated to serine and residues Arg190, Lys193, and Glu231 mutated to alanine using O (*44*). Model bias was removed using simulated annealing and the model was refined using rigid body refinement, initial grouped B-factor refinement and energy minimization (CNSsolve, *41*). A limited number of solvent molecules was built in using Arp (*45*). This included placement of a solvent molecule close to one of the crystallographic 2-fold axis and interacting with the mutation site (Figure 2b). The final model has good stereochemistry and an *R*-factor of 24.8% (R_{free} = 29.2%).

The coordinates of the wild-type and the mutant cofactor binding domains will be deposited in the Protein Data Bank.

Spectroscopic Techniques. Circular dichroism spectra were recorded on a Jasco J-720 spectropolarimeter. Far UV (190−250 nm) and near UV (250−310 nm) CD measurements

were performed at 20 °C in a 0.1 cm and in a 1.0 cm path length quartz cuvette, sealed with a Teflon stopper, at a protein concentration of 0.20 and 7.00 mg/mL, respectively. The results were expressed as mean residue ellipticity ([Θ]), assuming a mean residue weight of 110 per amino acid residue. Spectra were accumulated four times. All values were corrected for solvent contributions.

GdmCl and Urea Induced Equilibrium Unfolding. Protein samples were dialyzed against 20 mM sodium phosphate pH 7.0 and then incubated at 0.15 mg/mL final concentration at increasing concentrations of urea (0−7.9 M) or GdmCl (0−4.5 M) in 20 mM sodium phosphate pH 7.0. Far UV CD spectra were recorded after 24 h at 20 °C. To probe the reversibility of the unfolding process, the protein was unfolded at 20 °C in 4.5 M GdmCl or in 7.9 M urea at 1.5 mg/mL protein concentration in 20 mM sodium phosphate, pH 7.0. After 24 h, the refolding was started by 10-fold dilution of the unfolding mixture at 20 °C into solutions of the same buffer used for the unfolding containing decreasing denaturant concentrations. The final protein concentration was 0.15 mg/mL. After 2 h, a time that was established to be sufficient to reach equilibrium, far UV CD spectra were recorded at 20 °C. Equibibrium unfolding curves were analyzed by fitting baseline and transition regions simultaneously to a two-state linear extrapolation model as described before for the wild-type GluDH domain (*35*). Errors in $\Delta G_u H_2O$ are typically large due to the large extrapolation from the transition region to zero concentration denaturant. Averaged *m* values and $[\text{urea}]_{1/2}$ or $[\text{GdmCl}]_{1/2}$ values were therefore used to calculate the difference in unfolding free energy between wild-type and mutant proteins in the transition region as follows (*49*):

$$\Delta\Delta G_D = \langle m \rangle \Delta[\text{denaturant}]_{1/2} \quad (1)$$

in which $\Delta[\text{denaturant}]_{1/2}$ is the difference in the values of $[\text{denaturant}]_{1/2}$ between wild-type and mutant enzymes and $\langle m \rangle$ is the average value of *m*. The average *m* values determined in this study are 1.46 kcal mol^{-1} M^{-1} for urea unfolding and 2.96 kcal mol^{-1} M^{-1} for GdmCl induced unfolding. Because the mutation sites are fully exposed in the folded state, there is only a very small free energy difference for transfer from water to denaturant solution between wild-type and mutant folded and unfolded states, so that the free energy difference determined in the transition region equals $\Delta\Delta G_u^{H2O}$ (*49*, *10*).

Determination of Interaction Energies from Double Mutant Cycles. Interaction energies between two residues were determined by constructing double mutant cycles (*10*, *50*). A typical cycle consists of wild-type protein (E-XY), two single mutants (E-XM and E-MY) and the double mutant (E-MM). The free energy of interaction ($\Delta\Delta G_{int}$) between the 2 residues is then given by

$$\Delta\Delta G_{int} = \Delta G_D(_{E-XY>E-XM}) - \Delta G_D(_{E-MY>E-MM}) = \Delta G_D(_{E-XY>E-MY}) - \Delta G_D(_{E-XM>E-MM}) \quad (2)$$

The energies on the right-hand sight are the energies obtained from the urea and GdmCl induced denaturations as described above. In this study, the construction of a thermodynamic box (Figure 4) allowed the determination of the interaction energies between each two out of three residues in a salt-bridge triad in the presence as well as in the absence of the third residue analogous to the triple mutant box analysis on barnase (*10*).

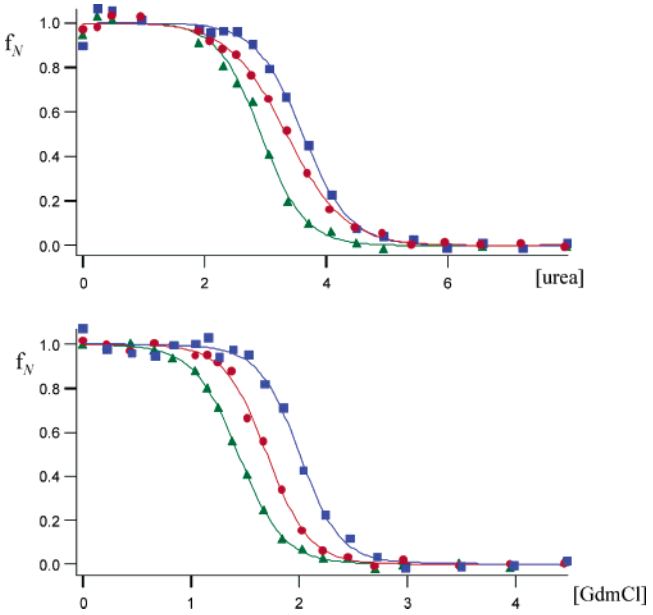

FIGURE 3: A selection of equilibrium unfolding curves for *T. maritima* GluDH cofactor binding wild-type and mutant proteins for (a) urea-induced unfolding and (b) GdmCl-induced unfolding. Arg190/Lys193/Glu231 (circles), mutant Ala190/Lys193/Ala231 (triangles), and mutant Arg190/Ala193/Glu231(squares). Depicted is the fraction of folded protein (f_N) as a function of denaturant concentration.

Thermal Equilibrium Unfolding. Protein samples were dialyzed against 20 mM sodium phosphate, pH 7.0, and thermal denaturation scans were recorded at 0.2 mg/mL and pH 7.0. The samples were heated from 10 to 95 °C and subsequently cooled to 10 °C with a heating/cooling rate ranging from 0.75 °C/min to 1.50 °C/min controlled by a Jasco programmable Peltier element. A scan rate of 1 °C/min was chosen in consideration of the observed independence of thermal transitions on the heating/cooling rate. Far UV CD spectra were recorded every 5−2.5 °C, and the dichroic activity at 222 nm was continuously monitored every 0.5 °C with 4 s averaging time. All the spectra were corrected for solvent contribution at increasing temperature. Reversible thermal denaturation was analyzed according to a two-state model as described for the wild-type GluDH cofactor binding domain (*35*). The differences in free energy between wild-type and mutant protein variants were obtained from

$$[T_m(\text{wt}) - T_m(\text{mut})][\Delta H_m(\text{wt})/T_m(\text{wt})] \quad (3)$$

and refer to a temperature between the T_m values of the wild-type and the respective mutant protein (*51*). The average error in T_m was 0.4 °C which corresponds to an error of approximately 0.06 kcal/mol in $\Delta\Delta G$ values. This is somewhat higher than the errors obtained from the chemical unfolding data, and because of this, we could not calculate significant interaction energies for the thermal unfolding data.

RESULTS

The Three-Dimensional Structure of the Wild-Type GluDH Cofactor Binding Domain. Comparison of the Wild-Type Domain to its Counterpart in the GluDH Hexamer. An

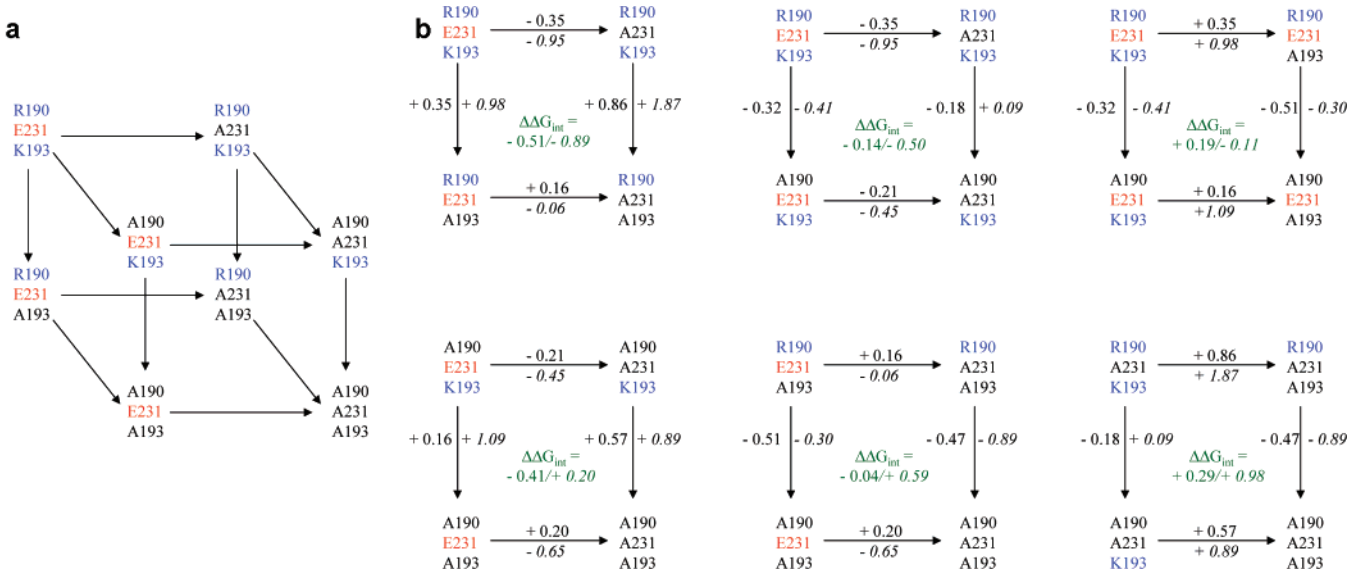

FIGURE 4: (a) Triple mutant box to determine interaction energies and cooperativity in salt-bridge triad Arg190−Glu231−Lys193. The single-letter notation for amino acids is used. Positively charged arginine and lysine are depicted in blue, negatively charged glutamate in red, and uncharged alanines in black. (b) Six mutant cycles used to construct the triple mutant box. The same color coding is used as in Figure a. $\Delta\Delta G_D$ is indicated next to the arrows, in plain numbers for urea unfolding, and in italic for GdmCl unfolding. $\Delta\Delta G_{int}$ is the interaction energy (green colored font) between the two residues analyzed in each particular cycle, again in plain numbers for urea and italic for GdmCl.

overlay of the models of the isolated cofactor binding domain determined in this study, with the cofactor binding domain of subunit A of the *T.maritima* GluDH hexamer, reveals local deviations at the N- and C-termini and at three loop regions that are all very close to the interface with the substrate binding domain (Figure 1). The side chains of Phe223 and Asn219, those in the hexamer pack against the substrate binding domain, have adopted new conformations. The two C-terminal residues Pro336 and Asp337 have shifted to pack closer to the cofactor binding domain. However, the overall folds of both domains are very similar (rmsd. of 0.956 Å), indicating that no significant structural changes have occurred upon isolated expression of the domain.

Description of the Salt-Bridge Triad Arg190−Glu231−Lys193. A three-residue ion-pair network is present in the domain, involving the side chains of arginine 190, glutamate 231, and lysine 193 (Figures 1 and 2, Table 2). Two ion-pair interactions are formed, one between the positively charged guanidino group of arginine and the negative γ-carboxylate group of glutamate (distance between Arg190 $N^{\eta 1}$ and Glu231 $O^{\epsilon 1}$ is 3.65 Å) and the second between the glutamate and the positively charged nitrogen of the lysine (distance between Glu231 $O^{\epsilon 1}$ and Lys193 N^{ζ} is 3.27 Å). Furthermore, Glu231 $O^{\epsilon 1}$ and Lys193 N^{ζ} form a hydrogen bond (Table 2). The distance between the positively charged groups Arg190 $N^{\eta 1}$ and Lys193 N^{ζ} is 5.36 Å, with a water molecule (W103) located between these two groups (Table 2). The central role of this water molecule is apparent from the fact that it donates a hydrogen to Glu231 $O^{\epsilon 1}$ and accepts hydrogens from Arg190 $N^{\eta 1}$ and Lys193 N^{ζ}. Lys193 N^{ζ} is furthermore donating a hydrogen to solvent molecule W19, so its hydrogen bonding capacity is fully used. The side chain of Arg190 is clearly adopting two conformations with similar occupancies. In the second conformation (B), the only interactions seem to be with W58 (2.73 Å from $BN^{\eta 1}$) and W122 (3.26 Å from $BN^{\eta 2}$). The aliphatic parts of the side chains of Lys193 and Arg190 participate in hydrophobic interactions with each other and with Leu232, Ile228, Leu227,Val194, and Phe223. The side chain of Glu231 also contributes by interacting with Leu227.

Table 2: Ionic Interactions and Hydrogen Bonds in the Salt-Bridge Triad[a]

Ionic Interactions		
Atom 1	Atom 2	Distance (Å)
Arg190 NH1	Glu231 OE1	3.65
Arg190 NH1	Glu231 OE2	3.80
Lys193 NZ	Glu231 OE1	3.27
Lys193 NZ	W2 Cl^-	3.33
Arg190 NH1	Lys193 NZ	5.36[b]

Hydrogen Bonds			
Donor	Acceptor	Distance D−A[c]	Distance H−A[c]
Arg190 NH1	W103 O	2.66	1.75
Lys193 NZ	Glu231 OE1	3.27	2.44
Lys193 NZ	W19 O	2.96	2.08
Lys193 NZ	W103 O	3.13	2.15
W103 O	Glu231 OE1	3.31	2.31

[a] Cutoff distances for classification as an ion pair is 4.0 Å. [b] Expected repulsive interaction. [c] D = donor, A = acceptor, H = proton. Cutoff values for D−A and H−A are 3.5 and 2.5 Å, respectively. Hydrogen bonds were analyzed using WHATIF (*47*). Interactions were analyzed according to the classification of solvent molecule W2 as a chloride and W19 and W103 as waters (see Materials and Methods).

Effects of the Cysteine to Serine Mutation. The presence of an exposed cysteine residue in the wild-type domain requires the use of reducing agents during purification, characterization and crystallization (*35*). To facilitate further experiments, the cysteine was replaced by a serine using site-directed mutagenesis. The resulting protein was purified, and its chemical and physical properties were compared to those of the wild-type domain (results not shown). Near and far UV CD spectra and the elution volume from a calibrated Superose 12 size-exclusion chromatography were identical. Similar midpoints of transition, *m*-values and free unfolding energies obtained by urea and guanidinium chloride -induced

Table 3: Urea Induced Equilibrium Unfolding

	$[urea]_{1/2}$ (M)[a]	m (kcal mol^{-1} M^{-1})[a]	ΔG_D (kcal/mol)[b]	$\Delta\Delta G_D$ (kcal/mol)[c]
Arg190/Lys193/Glu231	3.32	1.30	4.85	0.00
Ala190/Lys193/Glu231	3.10	1.70	4.53	−0.32
Arg190/Lys193/Ala231	3.08	1.60	4.50	−0.35
Arg190/Ala193/Glu231	3.56	1.39	5.20	+0.35
Ala190/Lys193/Ala231	2.96	1.53	4.32	−0.53
Ala190/Ala193/Glu231	3.21	1.33	4.69	−0.16
Arg190/Ala193/Ala231	3.67	1.42	5.36	+0.51
Ala190/Ala193/Ala231	3.35	1.42	4.89	+0.04

[a] Values were obtained by fitting the unfolding data as reported in Materials and Methods. [b] ΔG_D was calculated by multiplying the denaturant concentration $[urea]_{1/2}$ by 1.46, the average value of m (*49*). [c] Values of $\Delta\Delta G_D$ are calculated according to eq 1 and are relative to the free energy for unfolding of the wild-type domain. The average error in $[urea]_{1/2}$ was 0.01 M, which corresponds to 0.015 kcal/mol. In all proteins the cysteine is replaced by a serine residue

Table 4: GdmCl Induced Equilibrium Unfolding

	$[GdmCl]_{1/2}$ (M)[a]	m (kcal mol^{-1} M^{-1})[a]	ΔG_D (kcal/mol)[b]	$\Delta\Delta G_D$ (kcal/mol)[c]
Arg190/Lys193/Glu231	1.73	3.40	5.12	0.00
Ala190/Lys193/Glu231	1.59	2.63	4.71	- 0.41
Arg190/Lys193/Ala231	1.41	3.00	4.17	- 0.95
Arg190/Ala193/Glu231	2.06	2.74	6.10	+ 0.98
Ala190/Lys193/Ala231	1.44	3.08	4.26	- 0.86
Ala190/Ala193/Glu231	1.96	3.00	5.80	+ 0.68
Arg190/Ala193/Ala231	2.04	2.73	6.04	+ 0.92
Ala190/Ala193/Ala231	1.74	2.72	5.15	+ 0.03

[a] Values were obtained by fitting the unfolding data as reported in Materials and Methods. [b] ΔG_D was calculated by multiplying the denaturant concentration $[GdmCl]_{1/2}$ by 2.96, the average value of m (*49*). [c] Values of $\Delta\Delta G_D$ are calculated according to eq 1 and are relative to the free energy for unfolding of the wild-type domain. The average error in $[GdmCl]_{1/2}$ was 0.01 M, which corresponds to 0.015 kcal/mol. In all proteins the cysteine is replaced by a serine residue.

Table 5: Equilibrium Thermal Unfolding Assayed by Far UV Circular Dichroism

	ΔH_m (kcal/mol)[a]	T_m (°C)[a]	$\Delta\Delta G$ (kcal/mol)[b]
Arg190/Lys193/Glu231	52.4	69.5	0.00
Ala190/Lys193/Glu231	49.5	67.3	- 0.34
Arg190/Lys193/Ala231	41.0	68.4	- 0.17
Arg190/Ala193/Glu231	53.8	71.0	+ 0.23
Ala190/Lys193/Ala231	44.6	68.5	- 0.15
Ala190/Ala193/Glu231	53.2	67.5	- 0.31
Arg190/Ala193/Ala231	52.7	71.2	+ 0.26
Ala190/Ala193/Ala231	50.6	70.8	+ 0.20

[a] Values were obtained by fitting the thermal unfolding data as reported in Materials and Methods. [b] $\Delta\Delta G$ was calculated according to $\Delta\Delta G = [T_m(wt) - T_m(mut)][\Delta H_m(wt)/T_m(wt)]$ and refers to a temperature between the respective T_m values (*51*). The average error in T_m was 0.4 °C, which corresponds to approximately 0.06 kcal/mol. In all proteins the cysteine is replaced by a serine Residue.

reversible unfolding were obtained. Melting temperatures and denaturation enthalpies derived from thermal equilibrium unfolding assayed by far UV CD were identical. These results indicate that the cysteine to serine mutation has no significant effect on the stability of the protein. This domain variant was therefore used as reference "wild-type" in all the experiments described below.

Construction, Purification, and Structure Validation of Salt-Bridge Mutants. To study the role of the ion-pair network Arg190−Glu231−Lys193, all three residues were mutated to alanines in all combinations. In all cases this was done using the domain without the cysteine as template. All protein variants were overexpressed at the same high level as the wild-type and were purified according to the same procedure. For all variants identical size exclusion chromatograpy profiles were obtained (data not shown). No significant changes were observed in the far and near UV CD spectra of the mutants compared to the wild-type domain (data not shown), indicating an identical secondary structure content and a similar tertiary structure arrangement.

The Three-Dimensional Structure of Domain Variant Ala190/Ala193/Ala231. To analyze the structural effects of the mutations in more detail, domain variant Ala190/Ala193/Ala231 was crystallized and its three-dimensional structure solved. Crystals of the Ala190/Ala193/Ala231 mutant belong to space group $P4_12_12$ and diffracted below 2.5 Å using Cu κ_α radiation. The model was refined to 2.6 Å with carefull placement of a limited number of solvent molecules. The overall fold of Ala190/Ala193/Ala231 is identical to that of the isolated wild-type domain (rmsd. of 0.560 Å; Figure 1). An overlay of the mutated region with that of the wild-type domain shows identical conformations for the backbone and neighboring side chains (Figure 2). The removal of the salt-bridge triad therefore has had no structural consequences for the remainder of the protein.

Urea, Guanidinium Chloride, and Thermally Induced Reversible Unfolding. The Effect of Mutations on the Free Energies for GdmCl, Urea, and Thermally Induced Unfolding. The effect of the mutations on the free energies for unfolding were determined at 20 °C and neutral pH using urea and GdmCl induced equilibrium unfolding (Tables 3 and 4, Figure 3). Thermal equilibrium unfolding was used to obtain melting temperatures and to calculate differences in free unfolding energies between wild type and mutants that refer to a temperature that is between the respective melting temperatures of the wild-type and the mutant protein (Table 5).

The replacement of Arg190 with alanine (domain variant Ala190/Lys193/Glu231) lowers the free energy for unfolding of the domain in urea and GdmCl and by thermal unfolding to approximately the same extent (−0.32, −0.41, and −0.34 kcal/mol, respectively). The extent of the effect of replacing Glu231 with alanine (Arg190/Lys193/Ala231) depends on the denaturant but is destabilizing in all cases. The destabilization is most pronounced upon unfolding by GdmCl (−0.95 kcal/mol). However, in contrast to the effects of removal of the arginine and the glutamate, the mutation of Lys193 to alanine (Arg190/Ala193/Glu231) is in all cases stabilizing the domain, up to as much as 0.98 kcal/mol in GdmCl. The combination of the destabilizing mutations in Ala190/Lys193/Ala231 is destabilizing the domain, while combining a destabilizing and a stabilizing mutation in Arg190/Ala193/Ala231 is stabilizing the domain. The removal of two positively charged side chains in Ala190/Ala193/Glu231 is destabilizing in urea and thermal unfolding but stabilizing in GdmCl induced unfolding. At room temperature there is almost no net effect of the mutation of all three charges to alanine; there are only marginal differences between the free energies of the wild-type domain and mutant Ala190/Ala193/Ala231 either using urea or guanidinium chloride as denaturant. This mutant has however a

Table 6: Interaction Energies in the Salt-bridge Triad

	$\Delta\Delta G_{int}$ urea (kcal/mol)	$\Delta\Delta G_{int}$ GdmCl (kcal/mol)
Arg190-Glu231 in the presence of Lys193	−0.14	−0.50
Arg190-Glu231 in absence of Lys193	−0.04	+0.59
Lys193-Glu231 in the presence of Arg190	−0.51	−0.89
Lys193-Glu231 in absence of Arg190	−0.41	+0.20
Arg190-Lys193 in the presence of Glu231	+0.19	−0.11
Arg190-Lys193 in absence of Glu231	+0.29	+0.98

somewhat higher melting temperature than the wild type and a higher free energy for thermal unfolding at approximately 70 °C.

Analysis of Multiple Thermodynamic Cycles. Using multiple thermodynamic cycles (Figure 4; *49*, *10*), the energies from the interactions between Arg190, Glu231, and Lys193 obtained from GdmCl and urea-induced unfolding were separated from the changes in free energy due to the removal of interactions between these three residues and the rest of the protein (Table 6). Furthermore, the strength of each of the pairwise interactions could be assayed in the presence and the absence of the third residue.

The interaction energies between Lys193 and Glu231 in the intact salt-bridge triad are −0.51 kcal/mol for urea-induced unfolding and −0.89 kcal/mol when using GdmCl as denaturant. The strength of the interaction is reduced when the third residue Arg190 is absent. Actually, using GdmCl, the interaction destabilizes the protein by 0.20 kcal/mol in the absence of Arg190.

The interaction between Arg190 and Glu231 is not so strong as the one between the lysine and the glutamate, but still stabilizes the protein in the intact triad by 0.14 and 0.50 kcal/mol for urea and GdmCl, respectively. Again, the cooperativity in the network is apparent from the changes in interaction energy when Lys193 is absent. In the presence of urea the interaction energy between Arg190 and Glu231, in the absence of Lys 193, is not measurable, whereas in the presence of GdmCl this interaction is highly destabilizing.

The repulsive nature of the interaction between Lys193 and Arg190 is apparent from the strong destabilization both in urea and GdmCl in the absence of the mediating glutamate at position 231. In the presence of Glu231, the interaction is less destabilizing and even slightly stabilizing the domain in GdmCl.

Cooperativity in the network follows from the difference between the interaction energy of two residues in the presence and in the absence of the third residue and is −0.10 kcal/mol for urea and − 1.09 kcal/mol for GdmCl induced equilibrium unfolding.

DISCUSSION

Recently we described the expression and biophysical characterization of the isolated cofactor binding domain from *Thermotoga maritima* GluDH, with the aim of using it as a model system to study the thermodynamics of potential stabilizing ionic interactions in a protein from a hyperthermophilic organism (*35*). The advantage of using this model system is that it is derived from an enzyme that is very well studied; X-ray structures are available for homologues from mesophilic and (hyper)thermophilic organisms (*5*, *7*, *8*, *52*−*55*), and it has been used to study the role of large ion-pair networks in conferring thermostability (*15*, *17*−*19*).

Central in our approach of studying the role of ion-pair networks is the validation of experimental data by the determination of the X-ray structures of crucial mutant proteins. In earlier studies we have used X-ray analysis to assess that introduced charged residues, characterized by large and flexible side chains, nevertheless are in the correct conformation for formation of the anticipated ion-pair interactions (*15*, *19*). In the present study, the X-ray structure of the wild-type domain is essential in showing that the domain adopts the correct fold (when compared to its conformation as part of the hexameric GluDH), as suggested by far UV CD spectroscopy (*35*). Furthermore, it shows the presence of a salt-bridge network with surrounding solvent ions at high resolution. The structure of the Ala190/Ala193/Ala231 variant showed no structural changes upon mutation and validates the use of multiple thermodynamic cycles in order to separate the interactions within the network from changes in the free energy for unfolding upon mutation due to interaction of the salt-bridge members with the rest of the protein.

The crystals of the wild-type domain were grown in the presence of 3 M NaCl, conditions in which significant screening of electrostatic interactions is expected. Salt-bridge triad Arg190−Glu231−Lys193 is present at high ionic strength in the isolated domain, although the arginine side chain is found to adopt two alternative conformations. A comparison of T4 lysozyme structures determined at low, medium, and high ionic strength revealed no structural changes related to the differences in ionic strength and suggests that a crystal structure determined at high salt concentration is a good representation of the structure at low ionic strength (*56*). This suggests that the structure of the domain determined at 3 M NaCl can also be used to analyze interactions at low ionic strength, relevant to compare urea and thermal denaturation data on one hand versus GdmCl data on the other hand.

A further consequence of high salt crystallization conditions in our case is the observation of preferential ion binding by the presence of two high peaks ($>7\ \sigma$) in the electron density map that were assigned to chloride ions (CL2 and CL3). In addition, on the basis of several criteria (see materials and methods), solvent molecules W10, W31, and W103 could also be chloride ions. Preferential anion binding by positively charged groups on the protein surface could potentially stabilize the protein by reducing the repulsive effects between the positively charged groups and the introduction of favorable electrostatic interactions and might counteract the destabilizing effect of the screening of the electrostatic interactions by high salt concentrations. Preferential anion and cation binding has been described for several proteins isolated from halophilic organisms (*57*, *58*). These proteins have adapted to their high salt environment (up to supersaturating concentrations) by covering their surfaces with ion pairs and a large excess of negatively charged residues. Anion binding is also seen in T4 lysozyme where chloride ions are present at the termini of two helices that interact favorably with the helix dipole moment (*59*). It is remarkable that Lys193 is coordinating at least one chloride (CL2) but possibly a second (solvent molecule 103). Solvent molecule 103 is located centrally in the salt-bridge triad. This molecule being a chloride instead of a water would mean the loss of three hydrogen bonds, but the gain of a

more favorable electrostatic environment together with Arg190 and Lys193.

The interaction energies determined from unfolding data reflect the interactions in the folded state relative to their absence in the unfolded state. In the folded protein, each charged group is involved in short-range interactions with its partners in the salt bridge, as well as in long-range electrostatic interactions with other charges in the protein. For example, each of the three charged side chains might interact either favorably or unfavorably with existing α-helix dipoles in the protein. The aliphatic parts of all side chains are involved in hydrophobic interactions with neighboring hydrophobic residues. The measured unfolding free energy changes (but not the interaction energies determined by multiple thermodynamic cycles) therefore reflect the effect of disruption of multiple interactions and not only that of the ion-pair interactions. This is evident from the discrepancies between the changes in free energy for unfolding of the mutants and the determined ion-pair interaction energies (Tables 3 and 4 vs Table 6). While the removal of glutamate and arginine is destabilizing, the removal of the lysine side chain is actually stabilizing the domain. The net effect of replacing the salt bridge with hydrophobic residues is virtually zero at room temperature and slightly destabilizing at higher temperatures. The reason that we do not see a destabilization of the triple alanine mutant compared with the intact triad could in our case be due to hydrophobic effects because the alanine residues are introduced in an environment containing several other hydrophobic residues. The loss of favorable electrostatic interactions could furthermore be counteracted in the mutant by the higher α-helix stability of alanine residues compared to charged amino acids. While alanines are a good choice with respect to the analysis of thermodynamic cycles, they are not optimal representatives as surface residues. The exchange of the ion-pair network members to polar, uncharged residues might be a more suitable choice if only changes in free energies for unfolding are studied. Nevertheless, in the intact salt-bridge triad, both the interaction between glutamate and lysine and the interaction between glutamate and arginine are contributing favorably to the free energy for unfolding of the domain. In fact, the attractive ion-pair interactions are measured by chemical denaturation at 20 °C and should gain in stability by about 30% at the growth temperature of *Thermotoga*, due to the reduced desolvation penalty at higher temperatures (*3*, *13*). The interaction between Glu231 and Lys193 involves not only an ion pair but also a hydrogen bond and it is considerably stronger than the ion-pair interaction between Glu231 and Arg190, with the latter residue adopting two conformations. Identical results were described for barnase, where the exchange of a salt-bridge triad for alanines resulted in an unchanged free energy for unfolding but where stabilizing interaction energies where found between the network residues (*10*).

Earlier results we obtained regarding the role of ion-pair networks in determining the stability of *T. maritima* GluDH were the observation of cooperativity in a large ion-pair network at the subunit interface of the hexameric enzyme (*19*). Even though the characterization of this network was limited to addressing its role in kinetic stabilization because of irreversibility of the thermal unfolding reaction, it was obvious that the combination of three destabilizing single mutations Ser128Arg, Thr158Glu, and Asn117Arg resulted in a small but significant stabilization of the triple mutant compared to wild-type GluDH. While for the two central charged residues this was anticipated because of their intimate interaction across the subunit interface, the third mutation is located more than 15 Å away from the central charges in the network. Obviously there is cooperativity within this network, either exerted via subtle backbone shifts and/or via optimization of the overall electrostatic field present in this part of the protein. In this study we have shown that thermodynamic cooperativity is present in the Arg190−Glu231−Lys193 salt-bridge triad in the isolated cofactor binding domain. The cooperativity follows from the difference between interaction energies between two partners in the triad in the presence and in the absence of the third residue. The presence of a third residue strengthens each interaction by 0.10 kcal/mol in urea and as much as 1.09 kcal/mol in GdmCl. While the interaction energies as well as the cooperative effect are relatively small in urea, in GdmCl the effect of the third position residue makes a major difference. Each interaction in the absence of the third residue is significantly destabilizing the protein, while in the intact triad all interactions become stabilizing. Cooperativity between ion-pair interactions in barnase have thoroughly been analyzed and reported (*10*). From a molecular dynamics simulation on the DNA-binding protein Sac7d from the hyperthermophile *Sulfolobus acidocaldarius*, it was concluded that, rather than individual salt bridges, three large clusters provide most of the electrostatic stabilization toward thermal denaturation (*33*). Furthermore, some intercluster salt bridges in fact contribute unfavorably toward the stability of the folded state. In *Bacillus caldolyticus* cold shock protein, a 66-residue all-β protein, pairwise interactions between residues at positions 3, 46, and 66 in the protein sequence have been analyzed using a triple mutant cycle (*28*). Only two repulsive pairwise interactions are found in this triad, residues at positions 46 and 66 do not interact. The main stabilization of this protein comes from a favorable electrostatic contribution of arginine at position 3. However, the attractive electrostatic component is not localized in a pairwise interaction with any other surrounding residue. This might be related to the observation that many of the side chains involved adopt multiple conformations as visualized in the crystal structures of wild-type and several mutant proteins (*29*). No cooperativity was observed between these interactions.

The urea and thermal unfolding experiments were performed at low ionic strength and the obtained changes in free energy for unfolding are similar for both techniques (compare Table 3 and Table 4). This is in accordance with other studies (*60*−*62*). Guanidinium chloride, however, is a charged denaturant, and the unfolding free energies therefore reflect high ionic strength conditions. High ionic strength has been reported to significantly screen the electrostatic component of salt-bridge interactions (*10*, *60*). Interaction energies of salt bridges are therefore expected to be lower in GdmCl than in urea. This is obviously not the case for the isolated cofactor binding domain; both the changes in free energies for unfolding as well as the interaction energies are considerably larger in GdmCl induced unfolding. Interestingly, also the pairwise salt-bridge interaction between Glu14 and the N-terminus in rubredoxin from the hyper-

thermophilic archaeon *Pyrococcus furiosus*, derived from multiple thermodynamic cycles, was found to be twice as strong in GdmCl as in urea induced unfolding (*30*).

We stated that the interaction energies determined from unfolding data reflect the interactions in the folded state relative to their absence in the unfolded state. The central glutamate in the triad is far removed in sequence from the positively charged residues and it seems safe to assume that no interaction remains in the denatured state. However, it has been known for some time that under some conditions, the denatured state can be compact and may contain a considerable amount of residual structure (*63*). In particular, recent experiments provide evidence for the presence of charge−charge interactions in the denatured state (*61*, *62*, *64*). The domain denatured in GdmCl probably does not contain residual electrostatic interactions, since this denaturant has been reported to screen electrostatics. However, we cannot rule out the existence of residual electrostatic interactions in the denatured domain in the urea and thermal denaturation experiments. Whether this would result in lower interaction energies between the salt-bridge network residues during multiple thermodynamic cycles would depend on whether these interactions are still (partially) present in the denatured state.

It has furthermore been reported that GdmCl is under some conditions actually stabilizing proteins, in addition to acting as a denaturant. In the case of ribonuclease T1, the effect is small and attributed to cation binding in the native state (*65*). For ubiquitin the effect is characterized as binding of two chloride atoms by the native state of the protein, while the denatured state binds no anions (*66*). The stabilization of ubiquitin observed in 1 M GdmCl is remarkable and accompanied by an increase in melting temperature of 15 °C and in unfolding enthalpy of 12.5 kcal/mol. The stabilization is furthermore apparent from a comparison of the midpoints of denaturation in urea and GdmCl, while usually more urea is required to unfold a protein, ubiquitin has a midpoint for GdmCl denaturation almost 1 molar *higher* than for urea denaturation (*66*). The *T.maritima* cofactor binding domain as a whole is not stabilized by GdmCl to a large extent, the free energies for unfolding in GdmCl are in general only slightly higher than for urea. However, we cannot rule out local stabilization by anion binding in the vicinity of the ion-pair network that may be reflected in the higher interaction energies obtained by GdmCl denaturation, especially not since we observe that Lys193 is binding at least one and possibly two chloride atoms in the crystal structure.

In conclusion, we report here the first thermodynamic description of cooperativity in an ion-pair network in a protein from a hyperthermophile. Furthermore our results, together with results on a stabilizing salt bridge in hyperthermostable rubredoxin, not only show that hyperthermophiles use large cooperative arrangements of charged residue in order to stabilize their proteins, but also suggest that anion binding may have co-evolved with the presence of large ion-pair networks, to gain extra stability at high ionic strength conditions. Regarding the high internal ionic strength reported for several hyperthermophiles, among them *T. maritima* (*67*), this would actually be a logic strategy. However, this hypothesis requires further experimental validation, since it is in contrast with many observations that the strength of ionic interactions in general decreases in the presence of high salt concentrations.

ACKNOWLEDGMENT

We are very grateful to the staff of the EMBL outstation at the DESY synchrotron in Hamburg for providing the means of and help with data collection. We like to thank Gudrun Tibbelin and Majid Ali for their assistance in protein crystallization.

REFERENCES

1. Szilágyi, A., and Závodszky, P. (2000) Structural differences between mesophilic, moderately thermophilic and extremely thermophilic protein subunits: results of a comprehensive survey, *Structure 8*, 493−504.
2. Cambillau, C., and Claverie, J.-M. (2000) Structural and genomic correlates of hyperthermostability, *J. Biol. Chem. 275*, 32383−32386.
3. Karshikoff, A., and Ladenstein, R. (2001) Ion-pairs and the thermotolerance of proteins from hyperthermophiles: a 'traffic rule' for hot roads, *Trends Biochem. Sci.*, **26**, 550−556.
4. Kumar, S., and Nussinov, R. (2001) How do thermophilic proteins deal with heat? C*ell Mol. Life Sci. 58*, 1216−1233.
5. Yip, K. S., Stillman, T. J., Britton, K. L., Artymiuk, P. J., Baker, P. J., Sedelnikova, S. E., Engel, P. C., Pasquo, A., Chiaraluce, R., Consalvi, V., Scandurra, R., and Rice, D. W. (1995) The structure of *Pyrococcus furiosus* glutamate dehydrogenase reveals a key role for ion-pair networks in maintaining enzyme stability at extreme temperatures, *Structure*, *3*, 1147−1158.
6. Yip, K. S., Britton, K. L., Stillman, T. J., Lebbink, J., de Vos, W. M., Robb, F. T., Vetriani, C., Maeder, D., and Rice, D. W. (1998) Insights into the molecular basis of thermal stability from the analysis of ion-pair networks in the glutamate dehydrogenase family, *Eur. J. Biochem. 255*, 336−346.
7. Knapp, S., de Vos, W. M., Rice, D., and Ladenstein, R. (1997) Crystal structure of glutamate dehydrogenase from the hyperthermophilic eubacterium *Thermotoga maritima* at 3.0 Å resolution, *J. Mol. Biol. 267*, 916−932.
8. Britton, K. L., Yip, K. S. P., Sedelnikova, S. E., Stillman, T. J., Adams, M. W. W., Ma, K., Maeder, D. L., Robb, F. T., Tolliday, N., Vetriani, C., Rice, D. W., and P. J. Baker. (1999) Structure determination of the glutamate dehydrogenase from the hyperthermophile *Thermococcus litoralis* and its comparison with that from *Pyrococcus furiosus*, *J. Mol. Biol. 293*, 1121−1132.
9. Zhang, X., Meining, W., Fischer, M., Bacher, A., Ladenstein, R. (2001) X-ray structure analysis and crystallographic refinement of lumazine synthase from the hyperthermophile Aquifex aeolicus at 1.6 A resolution: determinants of thermostability revealed from structural comparisons, *J. Mol. Biol. 306*, 1099−1114.
10. Horovitz, A., Serrano, L., Avron, B., Bycroft, M., and Fersht, A. (1990) Strength and cooperativity of contributions of surface salt-bridges to protein stability, *J. Mol. Biol. 216*, 1031−1044.
11. Sali, D., Bycroft, M and Fersht, A. R. (1991) Surface electrostatic interactions contribute little to stability of barnase, *J. Mol. Biol. 220*, 779−788.
12. Dao-pin, S., Sauer, U., Nicholson, H., and Matthews, B. W. (1991) Contributions of engineered surface salt-bridges to the stability of T4 lysozyme determined by directed mutagenesis, *Biochemistry 30*, 7142−7153.
13. Elcock, A. H. (1998) The stability of salt-bridges at high temperatures: implications for hyperthermophilic proteins, *J. Mol. Biol. 284*, 489−502.
14. Tomschy, A., Bohm, G., and Jaenicke, R. (1994) The effect of ion pairs on the thermal stability of D-glyceraldehyde 3-phosphate dehydrogenase from the hyperthermophilic bacterium *Thermotoga maritima*, *Protein Eng. 7*, 1471−1478.
15. Lebbink, J. H. G., Knapp, S., van der Oost, J., Rice, D., Ladenstein, R., and de Vos, W. M. (1998) Engineering activity and stability of *Thermotoga maritima* glutamate dehydrogenase. I. Introduction of a six-residue ion-pair network in the hinge region, *J. Mol. Biol. 280*, 287−96.
16. Pappenberger, G., Schurig, H., and Jaenicke, R. (1997) Disruption of an ionic network leads to accelerated thermal denaturation of

D-glyceraldehyde-3-phosphate dehydrogenase from the hyperthermophilic bacterium *Thermotoga maritimaI*, *J. Mol. Biol. 274*, 676−683.
17. Rahman, R., Fujiwara, S., Nakamura, H., Takagi, M., and Imanaka, T. (1998) Ion-pairs involved in maintaining a thermostable structure of glutamate dehydrogenase from a hyperthermophilic archaeon, *Biochem. Biophys. Res. Commun. 248*, 920−926.
18. Vetriani, C., Maeder, D. L., Tolliday, N., Yip, K. S. P., Stillman, T. J., Britton, K. L., Rice, D. W., Klump, H. H., and Robb, F. T. (1998) Protein thermostability above 100 °C: a key role for ionic interactions, *Proc. Natl. Acad. Sci. U.S.A. 95*, 12300−12305.
19. Lebbink, J. H. G., Knapp, S., van der Oost, J., Rice, D., Ladenstein, R., and de Vos, W. M. (1999) Engineering activity and stability of *Thermotoga maritima* glutamate dehydrogenase. II. Construction of a 16-residue ion-pair network at the subunit interface, *J. Mol. Biol. 289*, 357−369.
20. Merz, A., Knöchel, T., Jansonius, J. N., and Kirschner, K. (1999) The hyperthermostable indoleglycerol phosphate synthase from *Thermotoga maritima* is destabilized by mutational disruption of two solvent-exposed salt-bridges, *J. Mol. Biol. 288*, 753−763.
21. Spassov, V. Z., Karshikoff, A. D., and Ladenstein, R. (1994) The optimization of the electrostatic interactions in proteins of different functional and folding type, *Protein Sci. 3*, 1556−1569.
22. Spassov, V. Z., Karshikoff, A. D., and Ladenstein, R. (1995) The optimization of protein solvent interactions. Thermostability and the role of hydrophobic and electrostatic interactions, *Protein Sci. 4*, 1516−1527.
23. Loladze, V., Ibarra-Molero, B., Sanchez-Ruiz, J. M., and Makhatadze, G. I. (1999) Engineering a thermostable protein via optimization of charge−charge interactions on the protein surface, *Biochemistry 38*, 16419−16423.
24. Spector, S., Wang, M., Carp, S. A., Robblee, J., Hendsch, Z. S., Fairman, R., Tidor, B., and Raleigh, D. P. (2000) Rational modification of protein stability by the mutation of charged surface residues, *Biochemistry 39*, 872−879.
25. Xiao, L., and Honig, B. (1999) Electrostatic contributions to the stability of hyperthermophilic proteins, *J. Mol. Biol. 289*, 1435−1444.
26. Kumar, S., Ma, B., Tsai, C.-J., and Nussinov, R. (2000) Electrostatic strengths of salt-bridges in thermophilic and mesophilic glutamate dehydrogenase monomers, *Proteins: Struct. Funct. Genet. 38*, 368−383.
27. Perl., D., Mueller, U., Heinemann, U., and Schmid, F. X. (2000) Two exposed amino acid residues confer thermostability on a cold shock protein, *Nat. Struct. Biol. 7*, 380−383.
28. Perl., D., and Schmid, F. X. (2001) Electrostatic stabilization of a thermophilic cold shock protein, *J. Mol. Biol. 313*, 343−357.
29. Delbrück, H., Mueller, U., Perl, D., Schmid, F. X., and Heinemann, U. (2001) Crystal structures of mutant forms of the *Bacillus caldolyticus* cold shock protein differing in thermal stability, *J. Mol. Biol*, *313*, 359−369.
30. Strop, P., and Mayo, S. L. (2000) Contribution of surface salt bridges to protein stability, *Biochemistry 39*, 1251−1255.
31. Horovitz, A., and Fersht, A. (1992) Co-operative interactions during protein folding, *J. Mol. Biol. 224*, 733−740.
32. Albeck, S., Unger, R., Schreiber, G. (2000) Evaluation of direct and cooperative contributions towards the strength of buried hydrogen bonds and salt bridges, *J. Mol. Biol. 298*, 503−520.
33. Bakker, P. I. W. de, Hünenberger, P. H., McCammon, J. A. (1999) Molecular dynamics simulation of the hyperthermophilic protein Sac7d from *Sulfolobus acidocaldarius*: Contribution of salt bridges to thermostability, *J. Mol. Biol. 285*, 1811−1830.
34. Lebbink, J. H. G., Eggen, R. I. L., Geerling, A. C. M., Consalvi, V., Chiaraluce, R., Scandurra, R., and de Vos, W. M. (1995) Exchange of domains of glutamate dehydrogenase from the hyperthermophilic archaeon *Pyrococcus furiosus* and the mesophilic bacterium *Clostridium difficile*: effects on catalysis, thermoactivity and stability, *Protein Eng. 8*, 1287−1294.
35. Consalvi, V., Chiaraluce, R., Gianciacomo, L., Scandurra, R., Christova, P., Karshikoff, A., Knapp, S., and Ladenstein, R. (2000) Thermal unfolding and conformational stability of the recombinant domain II of glutamate dehydrogenase from the hyperthermophile *Thermotoga maritima*, *Protein Eng. 13*, 501−507.
36. Ho, S. N., Hunt, H. D., Horton, R. M., Pullen, J. K., and Pease, L. R. (1989) Site-directed mutagenesis by overlap extension using the polymerase chain reaction, *Gene 77*, 51−59.
37. Gill, S. C., and von Hippel, P. H. (1989) Calculation of protein extinction coefficients from amino acid sequence data, *Anal. Biochem. 182*, 319−326.
38. Jancarik, J., and Kim, S.-H. (1991) Sparse matrix sampling: a screening method for crystallization of proteins, *J. Appl. Cryst. 24*, 409−411.
39. Otwinowski, Z., and Minor, W.(1997) Processing of X-ray diffraction data collected in oscillation mode, *Methods Enzymol. 276*, 307−326.
40. Navaza, J. (1994) AmoRe: an automated package for molecular replacement, *Acta Crystallogr., Sect A 50*, 157−163.
41. Brunger, A. T., Adams, P. D., Clore, G. M., Delano, W. L., Gros, P., Grosse-Kunstleve, R. W., Jiang, J.-S., Kuszewski, J., Nilges, M., Pannu, N. S., Read, R. J., Rice, L. M., Simonson, T.,Warren, G. L. (1998) Crystallography and NMR System, *Acta Crystallogr., Sect. D 54*, 905−921.
42. COLLABORATIVE COMPUTATIONAL PROJECT, NUMBER 4. (1994). "The CCP4 Suite: Programs for Protein Crystallography", *Acta Crystallogr., Sect. D 50*, 760−763.
43. Murshudov, G. N., Vagin A. A., and Dodson, E. J. (1997) Refinement of macromolecular structures by the maximum-likelihood method, *Acta Crystallogr., Sect. D 53*, 240−255.
44. Jones, T. A., Zou, J. Y., Cortan, J. Y., and Kjelgaard, M. (1991) Improved methods for building models in electron density maps and the location of errors in the model, *Acta Crystallogr., Sect. A, 47*, 110−119.
45. Perrakis, A., Morris, R. J. H., and Lamzin, V. S. (1999) Automated protein model building combined with iterative structure refinement, *Nat. Struct. Biol. 6*, 458−463.
46. Laskowski, R. A., MacArthur, M. W., Moss, D. S., and Thornton, J. M. (1993) PROCHECK: a program to check the stereochemical quality of protein structures, *J. Appl. Cryst. 26*, 283−291.
47. Vriend, G. (1990) WHAT IF: A molecular modeling and drug design program, *J. Mol. Graph. 8*, 52−56.
48. Hooft, R. W. W., Vriend, G., Sander, C., Abola, E. E. (1996) Errors in protein structures, *Nature 381*, 272−272.
49. Sali, D., Bycroft, M., and Fersht, A. R. (1988) Stabilization of protein structure by interaction of α-helix dipole with a charged side-chain, *Nature 335*, 740−743.
50. Serrano, L., Horovitz, A., Avron, B., Bycroft, M., and Fersht, A. (1990) Estimating the contribution of engineered surface electrostatic interactions to protein stability by using double-mutant cycles, *Biochemistry 29*, 9343−9352.
51. Pace, C. N. (1995) Evaluating contribution of hydrogen bonding and hydrophobic bonding to protein folding, *Methods Enzymol. 259*, 538−554.
52. Baker, P. J., Britton, K. L., Engel, P. C., Farrants, G. W., Lilley, K. S., Rice, D. W., Stillman, T. J. (1992) Subunit assembly and active site location in the structure of glutamate dehydrogenase, *Proteins: Struct., Funct. Gen. 12*, 75−86.
53. Peterson, P. E., Smith, T. J. (1999) The structure of bovine glutamate dehydrogenase provides insights into the mechanism of allostery, *Structure 7*, 769−782.
54. Smith, T. J., Peterson, P. E., Schmidt, T., Fang, J., and Stanley, C. A. (2001) Structures of bovine glutamate dehydrogenase complexes elucidate the mechanism of purine regulation, *J. Mol. Biol. 307*, 707−720.
55. Nakasako, M., Fujisawa, T., Adachi, S, Kudo, T., and Higuchi, S. (2001) Large-scale domain movement and hydration structure changes in the active-site cleft of unligated glutamate dehydrogenase from *Thermococcus profundus* studied by cryogenic X-ray crystal structure analysis and small-angle X-ray scattering, *Biochemistry 40*, 3069−3079.
56. Bell, J. A., Wilson, K. P., Zhang, X.-J., Faber, H. R., Nicholson, H., Matthews, B. W. (1991) Comparison of the crystal structure of bacteriophage T4 lysozyme at low, medium, and high ionic strengths, *Proteins: Struct. Funct. Gen. 10*, 10−21.
57. Frolow, F., Harel, M., Sussman, J. L., Mevarech, M., Shoham, M. (1996) Insights into protein adaptation to a saturated salt environment from the crystal structure of a halophilic 2Fe-2S ferredoxin, *Nat. Struct. Biol. 3*, 452−457.
58. Richard, S. B., Madern, D., Garcin, E., Zaccai, G. (2000) Halophilic adaptation: novel solvent protein interactions observed in the 2.9 and 2.6 Å resolution structures of the wild-type and a mutant of malate dehydrogenase from *Haloarcula marismortui*, *Biochemistry 39*, 992−1000.
59. Nicholson, H., Becktel, W. J., Matthews, B. W. (1988) Enhanced protein thermostability from designed mutations that interact with α-helix dipoles, *Nature 336*, 651−656.
60. Monera, O. D., ay, C. M., and Hidges, R. (1994) Protein denaturation with guanidine hydrochloride or urea provides a

different estimate of stability depending on the contributions of electrostatic interactions, *Protein Sci. 3*, 1984−1991.
61. Pace, C. N., Alston, R. W., and Shaw, K. L. (2000) Charge−charge interactions influence the denatured state ensemble and contribute to protein stability, *Protein Sci. 9*, 1395−1398.
62. Whitten, S. T., and Garcia-Moreno, B. (2000) Ph dependence of stability of staphylococcal nuclease: evidence of substantial electrostatic interactions in the denatured state, *Biochemistry 39* (46), 14292−14304.
63. Shortle, D. (1996) The denatured state (the other half of the folding equation) and its role in protein stability, *FASEB J. 10*, 27−34.
64. Kuhlman, B., Luisi, D. L., Young, P., and Raleigh, D. P. (1999) pK_a values and the pH dependent stability of the N-terminal domain of L9 as probes of electrostatic interactions in the denatured state. Differentiation between local and nonlocal interactions, *Biochemistry 38*, 4896−4903.
65. Mayr, L. M., and Schmid, F. X. (1993) Stabilization of a protein by guanidinium chloride, *Biochemistry 32*, 7994−7998.
66. Makhatadze, G. I., Lopez, M. M., Richardson, J. M., and Thomas, S. T. (1998) Anion binding to the ubiquitin molecule, *Protein Sci. 7*, 689−697.
67. Galinski, E. A. (1995) Osmoadaptation in bacteria, *Adv. Microb. Physiol. 37*:272−328.
68. DeLano, W. L. (2002) The PyMOL Molecular Graphics System on World Wide Web (http://www.pymol.org).

BI020461S